Asian Journal of Chemistry; Vol. 32, No. 9 (2020), 2375-2380

ASIAN JOURNAL OF CHEMISTRY

https://doi.org/10.14233/ajchem.2020.22578

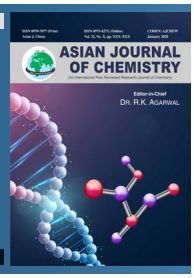

Citrus Extract Modified Graphene Oxide as a Green and Heterogeneous Organocatalyst for the Synthesis of Imidazole Derivatives

S. ARUNKUMAR[1,*], S. CHIDAMBARA VINAYAGAM[1,*], S. LAKSHMANAN[2] and S. ARUL ANTONY[1]

[1]Department of Chemistry, Presidency College, Chennai-600005, India
[2]Department of Chemistry, BIHER, Bharath University, Chennai-600073, India

*Corresponding author: E-mail: arunchemphd666@gmail.com

Received: 8 December 2019; *Accepted*: 23 July 2020; *Published online*: 20 August 2020; AJC-20041

A naturally benign convention was created with a surface change of graphene oxide by citrus extract as catalyst was prepared by a straight-forward chemical modification method. The prepared catalyst's catalytic activity was examined by the synthesis of imidazole derivatives at room temperature. It shows a strong acidic catalytic and sustainable organocatalyst. The prepared catalyst was characterized using different analytical procedures like elemental analysis, Fourier transforms infrared spectroscopy (FT-IR), powder X-ray diffraction (PXRD), energy-dispersive X-ray analysis (EDS), scanning electron microscopy images (SEM) and transmission electron microscopy images (TEM) analysis. The catalytic activity shows high activity and can be reused without significant loss of catalytic activity after five times. A present catalyst works easily under room temperature.

Keywords: Graphene oxide, Organocatalyst, Citric acid, Imidazoles.

INTRODUCTION

Among different nanomaterials graphene is a novel and carbon-based nanomaterials and also, it has pulled in as a result of its exceptional physical and chemical properties [1]. The unique properties of graphene are its high substance of carbon and oxygen proportion, its practical gathering change and surface properties were involving an appealing organocatalyst for biomedical applications for instance biosensor demonstrating, tranquilize conveyance and bacterial inhibition [2]. Recently, carbon materials are probably the best alternative for the generation of various organic compound synthesis. Because, they have extraordinary properties, for example, huge explicit surface area, high permeable structure and solid connections among carbon and hydrogen atoms. Thus, graphene oxide is a promising contender for a wide assortment of synergist applications [3]. Graphene oxide sheet have chemically reactive oxygen functional group, such as, carboxylic acid functionalities at their edges (as indicated by the generally known Lerf-Klinowski model) and hydroxyl and epoxy functionalities are available on the basal planes. Our definitive mean to do the chemical modification on graphene oxide sheets would use as an organocatalyst for many of the organic synthesis. For example, synthsis of amines (different types of nitrogens) on the graphene surface is one of the most widely recognized strategies for covalent functionalization. For instance of the utility of these functionalized materials, the expansion of long, aliphatic amine functionalities were exhibited to increase the activity on chemical reactions [4].

Imidazoles are classified in a fused heterocyclic and possessed a diverse range of pharmaceutical activities. Because of their potential and occurrence in nature, the ongoing exploration gave a few strategies need to made their subsidiaries and created many short approach for their amalgamation. These incorporate buildup of anthranilamide with aldehydes in nearness of acid, base catalysts and metal salts [5]. *N*-Bromo succinamide [6], $CuCl_2$ [7], silica chloride [8], K_3PO_4 [9], *etc*. catalysts demonstrated the limitations, for example, longer reaction time, encompassing conditions, homogeneous nature of the catalysts which makes the procedure tedious and exorbitant. However, aldehydes and ketone require more reaction times and delivering lowest yields. However, aldehydes and ketone require more reaction times and producing minimum yields. In such cases, poor yield were observed like aromatic

ketone is the major drawback of the imidazole synthesis. Acidic carbons, in light of the idea of greener blend, were accounted for as increasingly steady and high dynamic proton rich catalysts for a few acid based reactions. Graphene oxide and its alterations were successfully applied as heterogeneous catalyst for some organic reaction conversion [10]. Graphene is a slender type of carbon with various trademark, has been exceptional consideration on both the theoretical and practical applications in ongoing years [11].

In this work, on a fundamental level, graphene oxide was prepared from graphite as indicated by the modified Hummer′s method and then the prepared graphene oxide was scattered into the fluid citrus extract at room temperature and stirred overnight to get a heterogeneous organocatalyst, which was utilized in the synthesis of imidazole derivatives.

EXPERIMENTAL

Analytical reagent grade graphite powder, sodium nitrate, potassium permangnate, citric acid and hydrogen peroxide (30%) were purchased from Sigma-Aldrich and used without further purifications.

Synthesis of heterogeneous organocatalyst: Graphene oxide (GO) was synthesized from graphite powder using modified Hummer′s method [8], then citric acid modified graphene oxide was synthesized by the following procedure, 200 mg of graphene oxide was dispersed in 50 mL of water *via* sonication. To a dispersed solution, 50 mL of 10 M citric acid solution were added dropwise with constant stirring. The resultant solution was stirred at room temperature for 3 h and the obtained black precipitate was washed thoroughly and labeled as CA/GO [12].

Synthesis of imidazole derivatives: A mixture of organocatalyst (5 mg), 1 mmol of 2-aminobenzamide was stirred at 30 ºC for 10 min. Subsequently, corresponding aldehydes (1.2 mmol) was added. The resulting mixture was stirred at the same temperature until the reaction was completed. Then the catalyst was separated by simple filtration. The upper organic phase with the product was concentrated under reduced pressure. The crude products were purified by column chromatography (**Scheme-I**).

Spectral data

2-Phenyl-2, 3-dihydroquinazolin-4(1*H*)-one (3a): Yield: 90%; white solid, m.p. 178-180 ºC. ^{1}H NMR (300 MHz, DMSO) δ: 12.62 (s, 1H), 8.26 (dd, *J* = 8.8, 5.5 Hz, 2H), 8.17 (d, *J* = 8.0 Hz, 1H), 7.91-7.82 (m, 1H), 7.75 (d, *J* = 8.0 Hz, 1H), 7.60-7.50 (m, 1H), 7.41 (t, *J* = 8.8 Hz, 2H). ^{13}C NMR (75 MHz, DMSO) δ: 152.30 (s), 135.47 (s), 131.21 (d, *J* = 8.9 Hz), 128.13 (s), 127.45 (s), 126.69 (s), 116.61 (s), 116.32 (s), 41.19 (s), 40.92 (s), 40.64 (s), 40.36 (s), 40.08 (s), 39.80 (s), 39.52 (s). ES-MS (M+1) Calculated (*m/z*): 224.09. Anal. calcd. (found) % for $C_{14}H_{12}N_2O$: C, 74.98 (74.95); H, 5.39 (5.36); N, 12.49 (12.41).

2-(*p*-Tolyl)-2,3-dihydroquinazolin-4(1*H*)-one (3b): Yield: 81%; white solid, m.p. 184-186 ºC. ^{1}H NMR (300 MHz,

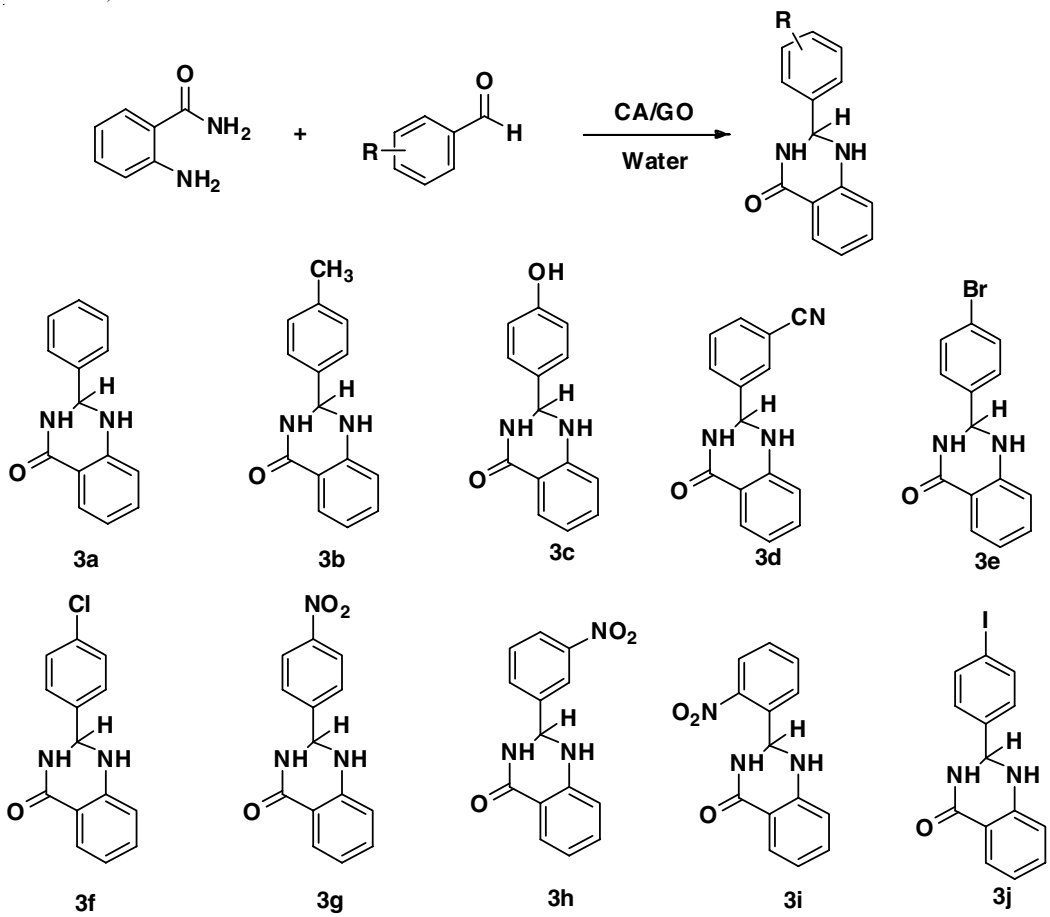

Scheme-I: CA/GO catalyzed imidazole derivative synthesis with different substitutions

DMSO) δ: 12.44 (s, 1H), 8.15 (d, *J* = 7.9 Hz, 1H), 7.83 (dd, *J* = 11.1, 4.2 Hz, 1H), 7.67 (d, *J* = 8.0 Hz, 1H), 7.51 (dd, *J* = 15.7, 7.8 Hz, 2H), 7.45-7.37 (m, 1H), 7.37-7.28 (m, 2H), 2.55-2.46 (m, 3H). ^{13}C NMR (75 MHz, DMSO) δ: 135.23 (s), 131.35 (s), 130.68 (s), 129.90 (s), 128.19 (s), 127.42 (s), 126.55 (d, *J* = 8.9 Hz), 41.37 (s), 41.09 (s), 40.81 (s), 40.63-39.82 (m), 39.70 (s), 20.33 (s). ES-MS (M+1) calculated (*m/z*): 238.11. Anal. Calcd. (found) % for $C_{15}H_{14}N_2O$: C, 75.61 (75.63); H, 5.92 (5.90); N, 11.76 (11.76).

2-(4-Hydroxyphenyl)-2,3-dihydroquinazolin-4(1*H*)-one (3c): Yield: 81%; white solid, m.p. 180-182 ºC. ^{1}H NMR (300 MHz, DMSO) δ: 12.41 (s, 1H), 8.14 (dd, *J* = 17.2, 8.4 Hz, 3H), 7.80 (t, *J* = 6.9 Hz, 1H), 7.69 (d, *J* = 7.8 Hz, 1H), 7.47 (t, *J* = 7.4 Hz, 1H), 7.07 (d, *J* = 8.9 Hz, 2H). ^{13}C NMR (75 MHz, DMSO) δ: 162.63 (s), 152.61 (s), 135.09 (s), 130.20 (s), 128.04 (s), 126.63 (d, *J* = 9.1 Hz), 125.66 (s), 114.66 (s), 80.13 (s), 79.69 (s), 79.27 (s), 56.16 (s), 41.26 (s), 40.98 (s), 40.70 (s), 40.28 (d, *J* = 20.7 Hz), 40.10-39.96 (m), 39.86 (s), 39.59 (s). ES-MS (M+1) calculated (*m/z*): 240.09. Anal. Calcd. (found) % for $C_{14}H_{12}N_2O_2$: C, 69.99 (69.91); H, 5.03 (5.02); N, 11.66 (11.68).

3-(4-Oxo-1,2,3,4-tetrahydroquinazolin-2-yl)benzonitrile (3d): Yield: 81%; white solid, m.p. 182-184 ºC. ^{1}H NMR (300 MHz, DMSO) δ: 12.64 (s, 1H), 8.29 (dd, *J* = 8.8, 5.5 Hz, 2H), 8.19 (d, *J* = 8.0 Hz, 1H), 7.94- 7.85 (m, 1H), 7.78 (d, *J* = 8.0 Hz, 1H), 7.64-7.53 (m, 1H), 7.44 (t, *J* = 8.8 Hz, 2H). ^{13}C NMR (75 MHz, DMSO) δ: 135.47 (s), 131.21 (d, *J* = 8.9 Hz), 127.45 (s), 126.69 (s), 116.61 (s), 116.32 (s), 41.19 (s), 40.92 (s), 40.64 (s), 40.36 (s), 40.08 (s), 39.80 (s), 39.52 (s). ES-MS (M+1) calculated (*m/z*): 249.27. Anal. calcd. (found) % for $C_{15}H_{11}N_3O$: C, 72.28 (72.30); H, 4.45 (4.46); N, 16.86 (16.88).

2-(4-Methoxyphenyl)-2,3-dihydroquinazolin-4(1*H*)-one (3e): Yield: 81%; white solid, m.p. 172-174 ºC. ^{1}H NMR (300 MHz, DMSO) δ: 12.41 (s, 1H), 8.12 (d, *J* = 6.7 Hz, 1H), 7.80 (d, *J* = 6.3 Hz, 1H), 7.70 (d, *J* = 6.1 Hz, 1H), 7.56 (s, 1H), 7.52-7.41 (m, 1H), 6.39 (s, 1H), 2.42 (s, 2H). ^{13}C NMR (75 MHz, DMSO) δ: 145.71 (s), 135.34 (s), 127.55 (s), 126.89 (s), 119.85 (s), 116.71 (s), 108.73 (s), 41.18 (s), 40.91 (s), 40.63 (s), 40.35 (s), 40.07 (s), 39.79 (s), 39.52 (s), 14.42 (s). ES-MS (M+1) calculated (*m/z*): 254.11. Anal. calcd. (found) % for $C_{15}H_{14}N_2O_2$: C, 70.85 (70.86); H, 5.55 (5.54); N, 11.02 (11.03).

2-(4-Chlorophenyl)-2,3-dihydroquinazolin-4(1*H*)-one (3f): Yield: 81%; white solid, m.p. 190-192 ºC. ^{1}H NMR (300 MHz, DMSO) δ: 12.60 (s, 1H), 8.15 (dd, *J* = 12.1, 8.4 Hz, 4H), 7.89-7.77 (m, 2H), 7.72 (d, *J* = 8.1 Hz, 1H), 7.60 (d, *J* = 8.6 Hz, 2H), 7.51 (t, *J* = 7.4 Hz, 1H). ^{13}C NMR (75 MHz, DMSO) δ: 162.63 (s), 152.61 (s), 135.09 (s), 130.20 (s), 128.04 (s), 126.63 (d, *J* = 9.1 Hz), 125.66 (s), 114.66 (s), 80.13 (s), 79.69 (s), 79.27 (s), 56.16 (s), 41.26 (s), 40.98 (s), 40.70 (s), 40.28 (d, *J* = 20.7 Hz), 40.10-39.96 (m), 39.86 (s), 39.59 (s). ES-MS (M+1) calculated (*m/z*): 258.06. Anal. calcd. (found) % for $C_{14}H_{11}N_2OCl$: C, 65.00 (65.02); H, 4.29 (4.28); N, 10.83 (10.84).

2-(4-Nitrophenyl)-2,3-dihydroquinazolin-4(1*H*)-one (3g): Yield: 81%; yellow solid, m.p. 196-198 ºC. ^{1}H NMR (300 MHz, DMSO) δ: 12.78 (s, 1H), 8.34 (d, *J* = 8.4 Hz, 2H), 8.18 (d, *J* = 7.3 Hz, 1H), 8.06 (t, *J* = 7.7 Hz, 2H), 7.84 (dt, *J* = 13.2, 7.9 Hz, 2H), 7.60 (dd, *J* = 16.2, 8.2 Hz, 1H). ^{13}C NMR (75 MHz, DMSO) δ: 133.37 (s), 129.47 (s), 41.19 (s), 40.77 (d, *J* = 20.9 Hz), 40.63-40.61 (m), 40.36 (s), 40.08 (s), 39.80 (s), 39.52 (s). ES-MS (M+1) calculated (*m/z*): 269.08. Anal. calcd. (found) % for $C_{14}H_{11}N_3O_3$: C, 62.45 (62.42); H, 4.12 (4.15); N, 15.61 (15.63).

2-(4-Nitrophenyl)-2,3-dihydroquinazolin-4(1*H*)-one (3h): Yield: 81%. ^{1}H NMR (300 MHz, DMSO) δ: 12.47 (s, 1H), 8.10 (dd, *J* = 15.4, 8.0 Hz, 3H), 7.82 (t, *J* = 7.6 Hz, 1H), 7.71 (d, *J* = 8.1 Hz, 1H), 7.49 (t, *J* = 7.4 Hz, 1H), 7.34 (d, *J* = 8.1 Hz, 2H). ^{13}C NMR (75 MHz, DMSO) δ: 142.27 (s), 135.33 (s), 130.82 (s), 130.00 (s), 128.52 (s), 127.17 (s), 126.67 (s), 120.94 (s), 41.36 (s), 41.08 (s), 40.81 (s), 40.53 (s), 40.25 (s), 39.97 (s), 39.69 (s), 21.80 (s). ES-MS (M+1) calculated (*m/z*): 269.08. Anal. calcd. (found) % for $C_{14}H_{11}N_3O_3$: C, 62.46 (62.45); H, 4.11 (4.11); N, 15.63 (15.64).

2-(2-Nitrophenyl)-2,3-dihydroquinazolin-4(1*H*)-one (3i): Yield: 81%; yellow solid, m.p. 190-192 ºC. ^{1}H NMR (300 MHz, DMSO) δ: 12.97 (d, *J* = 122.0 Hz, 1H), 8.77 (d, *J* = 5.9 Hz, 3H), 8.26-8.06 (m, 3H), 7.92-7.72 (m, 3H), 7.57 (dd, *J* = 10.8, 3.9 Hz, 1H). ^{13}C NMR (75 MHz, DMSO) δ: 151.56 (s), 151.10 (s), 135.55 (s), 128.56 (s), 128.17 (s), 126.78 (s), 122.45 (s), 42.65-41.29 (m), 41.19 (s), 40.77 (d, *J* = 21.1 Hz), 40.21 (d, *J* = 21.0 Hz), 39.80 (s), 39.51 (s). ES-MS (M+1) calculated (*m/z*): 269.08. Anal. calcd. (found) % for $C_{14}H_{11}N_3O_3$: C, 62.46 (62.46); H, 4.11 (4.11); N, 15.63 (15.63).

2-(4-Iodophenyl)-2,3-dihydroquinazolin-4(1*H*)-one (3j): Yield: 81%; white solid, m.p. 172-174 ºC. ^{1}H NMR (300 MHz, DMSO) δ: 12.97 (d, *J* = 122.0 Hz, 1H), 8.77 (d, *J* = 5.9 Hz, 3H), 8.26-8.06 (m, 3H), 7.92-7.72 (m, 3H), 7.57 (dd, *J* = 10.8, 3.9 Hz, 1H). ^{13}C NMR (75 MHz, DMSO) δ: 151.56 (s), 151.10 (s), 135.55 (s), 128.56 (s), 128.17 (s), 126.78 (s), 122.45 (s), 42.65-41.29 (m), 41.19 (s), 40.77 (d, *J* = 21.1 Hz), 40.21 (d, *J* = 21.0 Hz), 39.80 (s), 39.51 (s). ES-MS (M+1) calculated (*m/z*): 349.99. Anal. calcd. (found) % for $C_{14}H_{11}N_2O$: C, 48.02 (48.03); H, 3.17 (3.18); N, 8.00 (8.04).

RESULTS AND DISCUSSION

In present work, citrus extracted modified graphene oxide as a heterogeneous nanocatalyst was synthesized and utilized for the synthesis of imidazole derivatives under mild conditions in a short times. The graphene oxide was prepared *via* modified Hummer′s method further the citric acid was covalently bonded to graphene oxide nanosheets and then characterized by using several analytical techniques.

FTIR studies: FT-IR spectrum [Fig. 1A(i)] of modified graphene oxide revealed characteristic peaks at 1064 (C-O), 1273 (C-O-C), 1381 (C-OH) and 1726 (C=O), while the band at 1622 cm^{-1} can be attributed to the C=C vibration of oxidized graphene sheets [11,13]. The new peaks [Fig. 1A(ii)] appeared at 3350, 1627, 1315 and 779 cm^{-1} which are corresponds to O-H streching, C-H bending, C-H streching and O-H bending, respectively. The high intensity of 1627 cm^{-1} is due to the overlap of amide C=O stretching along with O-H bending.

EDX analysis: The EDX and elemental analysis confirmed that citric acid was coupled on the surface of graphene sheets and the results were also compared with oxidized graphene

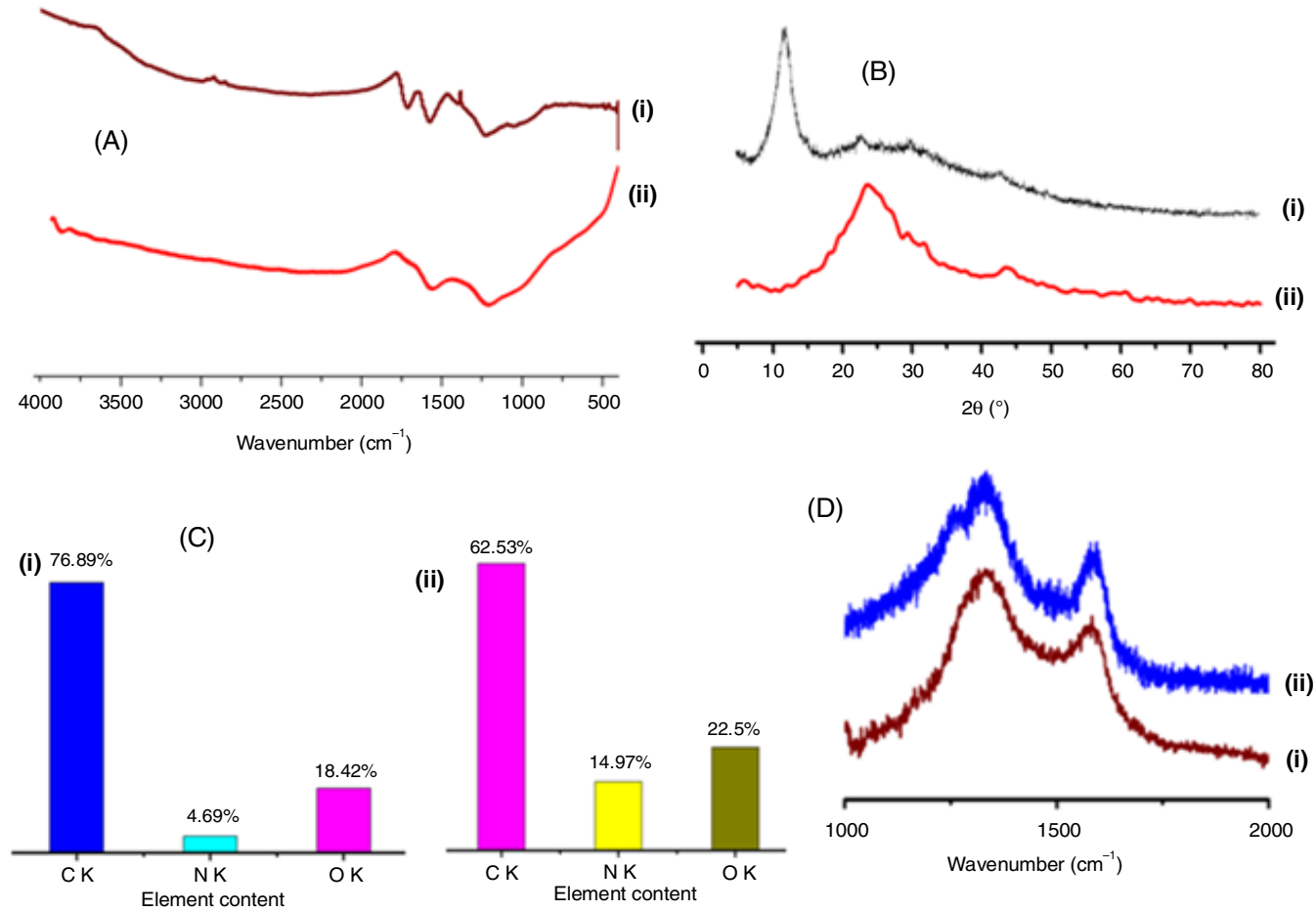

Fig. 1. FT-IR (A); PXRD (B); EDX (C) and Raman (D) spectrum of GO (i) and CA/GO (ii)

sheets [14]. The analyzed results show the carbon 76.89% and oxygen 18.42% in graphene oxide [Fig. 1C(i)], whereas Fig. 1C(ii) shows the composition of heterogeneous nanocatalyst, which consisted carbon 62.53% and oxygen 22.5%. EDX analysis clearly shows the presence of 22.5% of oxygen which indicated different types of oxygen were doped on the graphene sheets [15].

Graphene oxide and heterogeneous nanocatalyst were characterized by X-ray diffraction. It can be observed from Fig. 1B(i) that graphene oxide spectrum was appeared the sharp peak at 2θ = 12.3º, which is very close to the reported XRD pattern of graphene oxide [16]. On the other hand, after the citric acid treatment of graphene oxide, different types of modifications were observed on surface of graphene sheets. The XRD peak position shifted to 2θ = 26.1º similar to the XRD peak position of amine-graphene composite. This result illustrates the *d*-spacing of graphene oxide (*d* = 0.83 nm), which decreases after covalent treatment graphene sheets. This clearly indicates a significant number of oxygen groups was occurred on the surface of graphene oxide (*d* = 0.335nm) [17]. In addition, a peak of heterogeneous nanocatalyst at 2θ = 26.1º with broader width and weaker intensity than pristine graphene oxide (2θ = 12.3º) is due to the insertion of oxygen atom in to the graphene sheets. So the sheet was loss its crystal structure that means the degree of disorder increased with the oxidised graphene layers.

Raman analysis: The D and G bands are two intense Raman features in the spectra of materials. They were represented by peaks at around 1350-1320 and 1585-1570 cm^{-1}, respectively. In some cases, the peak called D′ also appeared at 1625-1602 cm^{-1}. The G-band is generally a doubly degenerated phonon mode of sp^2 carbon network and the 2D-band is the second-order Raman scattering process. However, due to the defects, a weak D-band determined at 1348 cm^{-1} is observed [18,19]. (Fig. 1D) shows the degree of structural deformations of the graphene oxide and heterogeneous nanocatalyst. The intensity ratio of D band to G band provides the different for the amount of structural defects between graphene oxide and heterogeneous nanocatalyst. The nanocatalyst was found to have an ID/IG ratio of 1.35, obviously larger than 0.91 observed for graphene oxide. The downshift of the G peak from graphene oxide in hetero-geneous nanocatalyst can be related to the electron rich oxygen group.

Morphological studies: The SEM images of the synthesized heterogeneous nanocatalyst and its precursor are presented in Fig. 2a-b. It is observed that a single sheet of graphene oxide is composed of a few layers which are loosely stacked on each other [20]. Whereas SEM image of heterogeneous nanocatalyst revealed that as-prepared catalyst consisted of randomly aggregated thin sheets which are closely associated, forming a porous and disordered network [21].

Fig. 3a shows the TEM image of graphene oxide with a crumpled silk like morphology, which is the characteristic

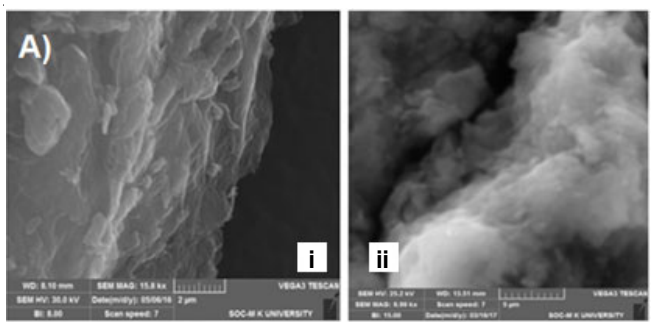

Fig. 2. SEM images of GO (a) and CA/GO (b)

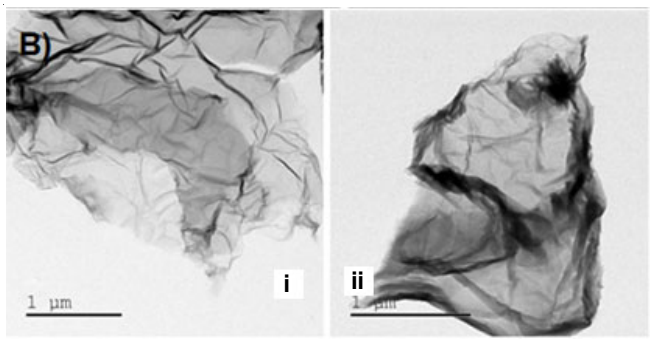

Fig. 3. TEM images of GO (a) and CA/GO (b)

feature of single layer of graphene sheets. As seen in Fig. 3b, TEM image of heterogeneous nanocatalyst in the graphene nanosheet has a typical crumpled surface with random stacking, which might be attributed to the defective structure formed upon exfoliation and the presence of foreign oxygen atoms [22].

Optimization of solvent: In order to identify a reliable solvent for the synthesized heterogeneous nanocatalyst catalyzed in the imidazole derivatives synthesis, a series of solvent such as ethanol, methanol, isopropanol, acetonitrile, tetrahydrofuran, 1,4-dioxane, toluene, ethanol:water, methanol: water and water were employed. The reaction was performed using organic solvents and the desired imidazoles with a good yield upto 77% (Table-1). To improve more benign nature of the carbocatalyst and practice greener protocols, the experiment was tried water as medium, the results were encouraging and excellent yield were observed up to 98% without further purification (entry 2, Table-1). Finally, water medium at room temperature was chosen as an optimum medium for the heterogeneous nanocatalyst for the catalyzed synthesis of compound **3a**.

Dosage of catalyst: Furthermore, catalyst load has a pivotal role in organic synthesis. Even though, the solvent and temperature optimization involve 10 mg of catalyst and further catalyst load optimization was carried out from 1 mg onwards (Fig. 4). It was observed that 5 mg of heterogeneous nanocatalyst is adequate for the complete conversion of the corresponding **3a**, with > 98% yield without any byproducts. Similarly, time optimization results also revealed that within 30 min, all the reactants were consumed and converted into the desired **3a**. Furthermore, the present catalytic system is highly specific towards the formation of **3a**, rather than other intermediate even in the presence of excess equivalence of reactants.

TABLE-1
SOLVENT OPTIMIZATION OF CA/GO CATALYZED IMIDAZOLE DERIVATIVE SYNTHESIS[a]

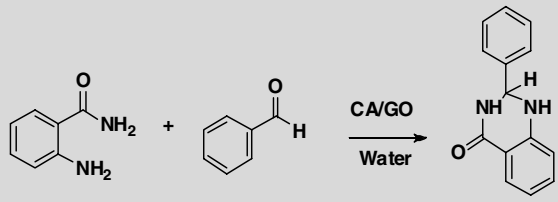

Entry	Solvent	Catalyst load (mg)	Yield[b] (%)
1	Ethanol	10	77
2	Water	10	98
3	Ethanol:water	10	73
4	Methanol:water	10	57
5	Methanol	10	53
6	Tetrahydrofuran	10	52
7	*iso*-propyl alcohol	10	72
8	Toluene	10	68
9	1,4-Dioxane	10	–
10	Ethyl acetate	10	70
11	Acetonitrile	10	68

[a]Reaction conditions: 2-Aminobenzamide (1 mmol), aldehydes (1.2 mmol), CA/GO catalyst (5 mg), solvent (5 mL), 0.5 h at room temp.; [b]All are isolated yield.

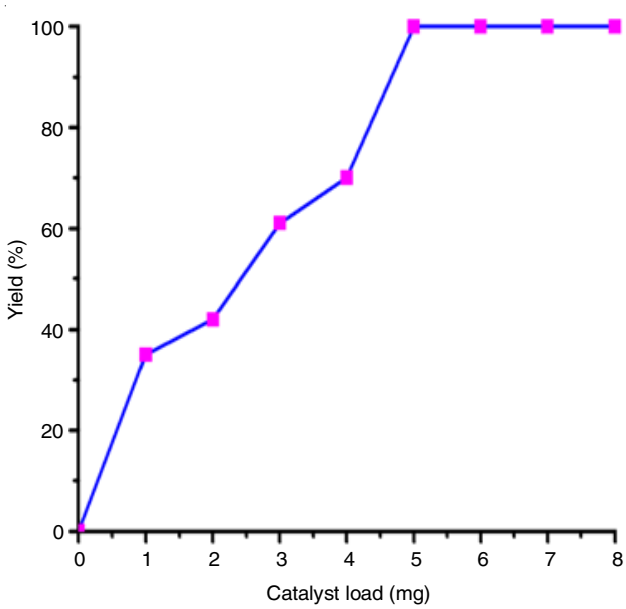

Fig. 4. Catalyst load optimization of CA/GO imidazole derivative synthesis

Reusability: The recyclability of as-prepared heterogeneous orangocatalyst (5 mg) was optimized in the reaction between 2-aminobenzamide (1 mmol) and aldehydes (1.2 mmol). After performing the first run, the reaction mixture was taken in water (5 mL) and after the reaction was completed as monitored by TLC. The catalyst was separated by using simple filtration and the filtered liquid containing product was isolated by vacuum distillation. The catalyst was then washed with methanol and acetone followed by drying to get the free floating heterogeneous orangocatalyst for further use. Recovered catalyst was little bit lower compared to the quantity used in the first run, which may be due to the loss of some acid functional groups involved in the reaction. However, the

reused catalyst was used for another five runs with almost equal efficiency and no significant change in the conversion (Fig. 5).

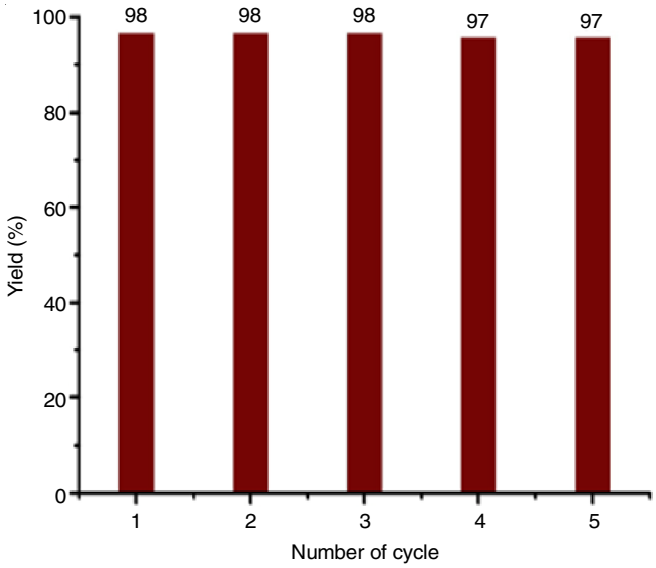

Fig. 5. Reusability and recovery of CA/GO in the model reaction

Conclusion

In summary, citric acid on graphene nanosheet was synthesized *via* simple chemical modification method. Efficient, imidazole derivatives were preceded over metal-free, citric acid graphene nanosheets under mild conditions. The surface analysis for a prepared heterogeneous orangocatalyst demonstrates that the graphene oxide was well functionalized with citric acid. The citric acid-grafted graphene oxide displayed a superior acidic behaviour and exhibited remarkable catalytic activity. Sustainable nature of the catalyst is very high and more stable even after few cycles.

CONFLICT OF INTEREST

The authors declare that there is no conflict of interests regarding the publication of this article.

REFERENCES

1. S. Nasir, M.Z. Hussein, Z. Zainal and N.A. Yusof, *Materials*, **11**, 295 (2018); https://doi.org/10.3390/ma11020295
2. M.J. Mphahlele, M.M. Maluleka and T.A. Khoza, *Bull. Chem. Soc. Ethiop.*, **28**, 81 (2014); https://doi.org/10.4314/bcse.v28i1.10
3. R.J. Abdel-Jalil, W. Voelter and M. Saeed, *Tetrahedron Lett.*, **45**, 3475 (2004); https://doi.org/10.1016/j.tetlet.2004.03.003
4. G.-Z. Li, R.K. Randev, A.H. Soeriyadi, G. Rees, C. Boyer, Z. Tong, T.P. Davis, C.R. Becer and D.M. Haddleton, *Polym. Chem.*, **1**, 1196 (2010); https://doi.org/10.1039/c0py00100g
5. H. Kabashima, H. Tsuji, T. Shibuya and H. Hattori, *J. Mol. Catal. Chem.*, **155**, 23 (2000); https://doi.org/10.1016/S1381-1169(99)00316-7
6. A. Villa, J.-P. Tessonnier, O. Majoulet, D.S. Su and R. Schlögl, *Chem. Commun.*, 4405 (2009); https://doi.org/10.1039/b906123a
7. Z.S. Wu, W. Ren, L. Xu, F. Li and H.M. Cheng, *ACS Nano*, **5**, 5463 (2011); https://doi.org/10.1021/nn2006249
8. W. Hummers Jr. and R. Offeman, *J. Am. Chem. Soc.*, **80**, 1339 (1958); https://doi.org/10.1021/ja01539a017
9. W. Wan, F. Zhang, S. Yu, R. Zhang and Y. Zhou, *New J. Chem.*, **40**, 3040 (2016); https://doi.org/10.1039/C5NJ03086B
10. M. Khan, E. Yilmaz, B. Sevinc, E. Sahmetlioglu, J. Shah, M.R. Jan and M. Soylak, *Talanta*, **146**, 130 (2016); https://doi.org/10.1016/j.talanta.2015.08.032
11. C.C. Yeh and D.H. Chen, *Appl. Catal. B*, **150-151**, 298 (2014); https://doi.org/10.1016/j.apcatb.2013.12.040
12. A. Maleki, Z. Hajizadeh and H. Abbasi, *Carbon Lett.*, **27**, 42 (2018).
13. F. Chen, L. Guo, X. Zhang, Z.Y. Leong, S. Yang and H.Y. Yang, *Nanoscale*, **9**, 326 (2017); https://doi.org/10.1039/C6NR07448K
14. M.M. Islam, S.N. Faisal, A.K. Roy, S. Ansari, K. Konstantinov, D. Cardillo and E. Haque, *J. Nanotechnol. Mater. Sci.*, **2**, 1 (2015); https://doi.org/10.15436/2377-1372.15.006
15. D. Li, C. Yu, M. Wang, Y. Zhang and C. Pan, *RSC Adv.*, **4**, 55394 (2014); https://doi.org/10.1039/C4RA10761F
16. R. Yadav and C.K. Dixit, *J. Sci. Adv. Mater. Dev.*, **2**, 141 (2017); https://doi.org/10.1016/j.jsamd.2017.05.007
17. H. Wang, T. Maiyalagan and X. Wang, *ACS Catal.*, **2**, 781 (2012); https://doi.org/10.1021/cs200652y
18. D. Guo, R.B. Song, H.H. Shao, J.R. Zhang and J.J. Zhu, *Chem. Commun.*, **53**, 10738 (2017); https://doi.org/10.1039/C7CC90353G
19. J. Balamurugan, S.G. Peera, M. Guo, T.T. Nguyen, N.H. Kim and J.H. Lee, *J. Mater. Chem. A*, **5**, 17896 (2017); https://doi.org/10.1039/C7TA04807F
20. M. Du, J. Sun, J. Chang, F. Yang, L. Shi and L. Gao, *RSC Adv.*, **4**, 42412 (2014); https://doi.org/10.1039/C4RA05544F
21. J. Long, X. Xie, J. Xu, Q. Gu, L. Chen and X. Wang, *ACS Catal.*, **2**, 622 (2012); https://doi.org/10.1021/cs3000396
22. A. Yang, J. Li, C. Zhang, W. Zhang and N. Ma, *Appl. Surf. Sci.*, **346**, 443 (2015); https://doi.org/10.1016/j.apsusc.2015.04.033